Hydrostatic relaxation scheme for the 1D shallow water - Exner equations in bedload transport

Putu Harry Gunawan[a,b,*], Xavier Lhébrard[b]

[a] *Industrial and Financial Mathematics Research Group, Faculty of Mathematics and Natural Sciences, Institut Teknologi Bandung, Jalan Ganesha 10, Bandung 40132, Indonesia.*

[b] *Universitée Paris-Est, LAMA UMR8050, F-77454, Marne-la-Vallée, France.*

Abstract

This paper describes the numerical scheme of the one-dimensional Exner - shallow water equations for sediment modelling. Here, our novel numerical scheme is called hydrostatic relaxation scheme which is a robust and straightforward scheme. This scheme is given as the hydrostatic reconstruction of the relaxation solver. Some numerical tests are presented such as analytical solution, transcritical flow over a granular bump, and erodible bottom due to dam-break. The comparisons of numerical and data experiments are also given in dam-break over granular bed simulation. The results of our simulation have a good agreement with analytical solution and the data experiments. Moreover, satisfactory convergence rate in L^1-norm is obtained.

Keywords: Shallow water equations, Exner equation, Bedload sediment,

*Corresponding author. Tel. +62 87 76 24 34 08 1

Email addresses: putu-harry.gunawan@u-pem.fr; harry.gunawan.putu@gmail.com (Putu Harry Gunawan), xavier.lhebrard@u-pem.fr (Xavier Lhébrard)

[1]The first author acknowledge the support of the Ensemble Estimation of Flood Risk in a Changing Climate project funded by The British Council through their Global Innovation Initiative, the scholarship support from DIKTI, and wish to thanks to François Bouchut for the valuable advise and for the great discussions.

Hydrostatic reconstruction, Relaxation solver, Dam-break.

1. Introduction

Sediment transport is an important phenomena in nature but least understood processes and complex, e.g. the morphological change under the actions of flooding, rain runoff, wave currents, and tidal flow. The flood can cause the biggest disasters to our environment such as erosion and deposition process. Hence the study of interaction between the flow and the transport dynamics and how this relation influence the morphology surface change are needed.

The numerical simulation of sediment process becomes important. However, the reliability of numerical result relies on how the mathematical model described the sediment process. Therefore, the accuracy of the governing equations and discretization of numerical scheme are required. Moreover, the numerical results still need to be verified and validated using analytical solution or data experiment to see the applicability of the scheme.

Some models and numerical approaches for sediment transport have been demonstrated Wu & Wang (2007); Capart & Young (1998); Simpson & Castelltort (2006); Cao et al. (2004); Cordier et al. (2011); Audusse et al. (2012). Some of them are quite complex because they consider physical characteristics of sediment in detail. In addition, their models include some type of sediment such as bedload and suspended load. For example, one of the simple model is called shallow water-Exner equations to study the bedload sediment transport and is introduced in Cordier et al. (2011), and Audusse et al. (2012).

The shallow water - Exner equations consists of three equations: mass conservation, momentum conservation and Exner equation which is a mass conservation of sediment in interaction with the fluid flow. In order to approximate this model, some methods are already studied such as splitting and coupled method. In splitting method, shallow water equations and Exner equation are computed separately. First, the shallow water equations can be approximated by the finite volume method using collocated approach (see Audusse et al. (2004); Greenberg & Leroux (1996); LeVeque (1998); Tang et al. (2004); Tao & Xu (1999)) or staggered approach (Doyen & Gunawan (2014); Stelling & Duinmeijer (2003); Herbin et al. (2014)) and afterward the Exner equation can be computed by a simple finite difference method.

However, splitting method using finite volume collocated approach seems not a robust scheme for shallow water - Exner equations (see Cordier et al. (2011)). In Cordier et al. (2011), they show that the splitting method fails to approximate shallow water - Exner equations because of the instability issue. Hence, they proposed coupled Roe scheme which is shown as a stable and robust scheme. Moreover, another coupled scheme is also introduced by Audusse et al. (2012), where the relaxation flux and simple solver are used to obtain some robust results as their expected.

Here we introduce a novel method, which is the combination of hydrostatic reconstruction and relaxation flux solver. The idea of this method is follow the paper of Audusse et al. (2004) and the book of Bouchut (2004). We apply the local hydrostatic reconstruction to determine a well-balanced scheme from the numerical flux of Audusse et al. (2012). According Audusse et al. (2004), the hydrostatic reconstruction method is designed to be applied

with a numerical flux for the homogeneous problem. However, here the numerical flux we used is for the non-homogeneous problem (i.e non-flat topography and friction). Moreover, we applied the apparent topography method for treatment the friction term, which is introduced in Bouchut et al. (2004). In order to validate the numerical results, we compared our results with the analytical solution and data experiments obtained in Berthon et al. (2012) and Capart & Young (1998) respectively. The comparison of data experiments and numerical computations is given in dam-break flow over granular bed simulation.

The outline of this paper is following: in Section 2, the model of coupled system shallow water and Exner equations are introduced. The discretization of numerical method such as hydrostatic reconstruction and relaxation flux solver described in Section 3. Some numerical tests and comparisons with analytical solution and data experiments are given in the Section 4. Last in Section 5, the conclusions are constructed.

2. Governing equations

2.1. The shallow water - Exner model

The one-dimensional coupled model of shallow water - Exner equations is given by

$$\partial_t h + \partial_x(hu) = 0 \tag{1}$$

$$\partial_t(hu) + \partial_x\left(hu^2 + \frac{1}{2}gh^2\right) + gh\partial_x Z = -ghS_f \tag{2}$$

$$\Phi\partial_t Z + \partial_x Q_s = 0 \tag{3}$$

where h is the total water depth, u is the velocity in the x direction, $Z = (z - H)$ is the bed elevation and H the depth of fixed bedrock layer to the reference level (see Fig. 1). The friction term is defined by S_f, $\Phi = (1 - \phi)$ with ϕ is the bed sediment porosity, Q_s is the bed load and g is the acceleration due to gravity.

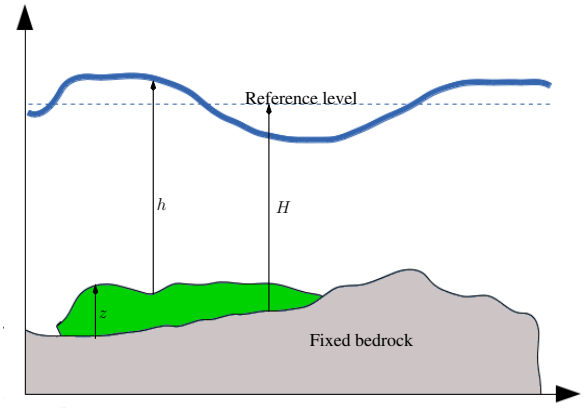

Figure 1: The one-dimensional sketch of shallow water with a sediment layer.

Some estimations for the sediment discharge Q_s have been obtained by empirical formulas. Some of most important empirical formulas of the bed load exist, such as Grass formula, Meyer-peter and Müller's formula or Van Rijn's formula (see Cordier et al. (2011); Van Rijn (1984); Rijn (1984) for more detail).

The Grass formula for the solid transport discharge are given as,

$$Q_s = A_g(u)|u|^{m-1}u \tag{4}$$

where A_g is a constant depending on the sediment properties (such as the grain diameter, cinematic viscosity, etc) and the experimental data, u is the

horizontal velocity of fluid, and the parameter $1 \leq m \leq 4$ is a given number depend on sediment. The value $m = 3$ is the usual value for the exponent m. The interval value A_g is such that $0 \leq A_g \leq 1$. If the value closed to 0, it means the interaction between the fluid and the sediment is weak. Meanwhile, the strong interaction between fluid and sediment is described with the value of A_g closed to 1.

For the friction terms, we consider the friction slope which depends on flow conditions (Simpson & Castelltort (2006); Kadlec (1990); Julien & Simons (1985)). Here we can use either Manning's friction law

$$S_f = \frac{\mu^2 u|u|}{h^{4/3}} \tag{5}$$

or Darcy-Weisbach's friction law

$$S_f = \frac{C_f u|u|}{8gh} \tag{6}$$

where μ is Manning's roughness coefficient, and C_f is the Darcy-Weisbach friction factor which depends on the Reynolds number. In this work, the coefficients μ and C_f are set to be constant. Note that, the friction law (5) is often used for the case when flow is laminar, and the later friction slope (6) is often used for the case when flow is turbulent in overland flow.

The empirical formula for the sediment discharge by Meyer-peter and Müller's is given by

$$Q_s = \text{sgn}(u) 8(\tau_* - \tau_{*c})^{3/2} \sqrt{(\phi_r - 1) g d^3}, \tag{7}$$

where g is gravitational force, d is the diameter size of sediment grain, $\phi_r = \rho_s/\rho_w$ is a relative density of fluids, ρ_w and ρ_s are the density of fluid and sediment respectively, τ_* is the non-dimensional shear stress and τ_{*c} is the

non-dimensional critical shear stress (see Cao et al. (2006) for more detailed). The non-dimensional shear stress τ_* is defined by

$$\tau_* = \frac{\tau}{(\gamma_s - \gamma)d}, \tag{8}$$

where $\tau = \gamma R_h |S_f|$ is the shear stress, $\gamma = g\rho_w$ denotes the specific weight of fluid, $\gamma_s = g\rho_s$ denotes the specific weight of the sediment, $R_h \approx h$ is the hydraulic ratio and S_f is the friction slope defined as (5) or (6) depends on type of water flow.

3. Numerical method

3.1. The 1D numerical scheme

We consider a grid of points $x_{i+\frac{1}{2}}$, $i \in \mathbb{Z}$, $\cdots < x_{-\frac{1}{2}} < x_{\frac{1}{2}} < \cdots$ and we define the cells and their lengths

$$\Omega_i = [x_{i-\frac{1}{2}}, x_{i+\frac{1}{2}}] \quad \Delta x_i = x_{i+\frac{1}{2}} - x_{i-\frac{1}{2}} > 0. \tag{9}$$

We shall define the discrete times by $t^n = n\Delta t, \quad n \in \mathbb{N}$ with a constant time step $\Delta t > 0$. Here we would like to approximate the solution of Eqs. (1) - (3), by discrete values $U_i^n = (h_i^n, h_i^n u_i^n, Z_i^n)^T, i \in \mathbb{Z}, n \in \mathbb{N}$. The discrete value U_i^n is computed by considering the averages of the exact solution over the cells,

$$U_i^n \approx \frac{1}{\Delta x_i} \int_{\Omega_i} U(t^n, x)\, \mathrm{d}x. \tag{10}$$

Then we can write the scheme as

$$U_i^{n+1} = U_i^n - \vec{\xi} \frac{\Delta t}{\Delta x_i} \left(F_{i+\frac{1}{2}L} - F_{i-\frac{1}{2}R} \right), \tag{11}$$

where $\vec{\xi} = [1, 1, 1/\Phi]^T$.

The fluxes are defined by hydrostatic reconstruction scheme as

$$F_{i+\frac{1}{2}L} = \mathcal{F}(U^n_{i+\frac{1}{2}L}, U^n_{i+\frac{1}{2}R}) + \begin{pmatrix} 0 \\ \frac{g(h^n_i)^2}{2} - \frac{g(h^n_{i+\frac{1}{2}L})^2}{2} \\ 0 \end{pmatrix}, \tag{12}$$

$$F_{i-\frac{1}{2}R} = \mathcal{F}(U^n_{i-\frac{1}{2}L}, U^n_{i-\frac{1}{2}R}) + \begin{pmatrix} 0 \\ \frac{g(h^n_i)^2}{2} - \frac{g(h^n_{i-\frac{1}{2}R})^2}{2} \\ 0 \end{pmatrix} \tag{13}$$

with $\mathcal{F}$ is a numerical flux which is defined by relaxation solver of shallow water - Exner equations introduced by Audusse et al. (2012) and will be recalled in next Subsection 3.3. Moreover, the reconstructed states $U_{i+\frac{1}{2}L}$ and $U_{i+\frac{1}{2}R}$ are defined by

$$U_{i+\frac{1}{2}L} = (h^n_{i+\frac{1}{2}L}, h^n_{i+\frac{1}{2}L}u^n_i, Z^n_i)^T, \tag{14}$$

$$U_{i+\frac{1}{2}R} = (h^n_{i+\frac{1}{2}R}, h^n_{i+\frac{1}{2}R}u^n_{i+1}, Z^n_{i+1})^T, \tag{15}$$

where

$$h_{i+\frac{1}{2}L} = (h^n_i - (\Delta Z)_+)_+, \tag{16}$$

$$h_{i+\frac{1}{2}R} = (h^n_{i+1} - (-\Delta Z)_+)_+, \tag{17}$$

$$\Delta Z = Z^n_{i+1} - Z^n_i, \tag{18}$$

with the notation $a_+ = \max(a, 0)$ and $Z^n_{i+1} = (z^n_{i+1} - H_{i+1})$.

3.2. Apparent topography

The source term (i.e friction term) in momentum conservation (2) is treated by apparent topography. This method was introduced by Bouchut

(2004) and some applications can be found in Delestre et al. (2013) and Delestre (2010).

To discretize the friction terms Eqs. (5) and (6), we define

$$\Delta F_{i+\frac{1}{2}} = f^n_{i+\frac{1}{2}} \Delta x_i, \tag{19}$$

where $f^n_{i+\frac{1}{2}}$ for Manning's is given as

$$f^n_{i+\frac{1}{2}} = \begin{cases} 0 & \text{if } h_i = h_{i+1} = 0, \\ \dfrac{\mu^2 u^n_{i+\frac{1}{2}} |u^n_{i+\frac{1}{2}}|}{(h^n_{i+\frac{1}{2}})^{4/3}} & \text{otherwise.} \end{cases}, \tag{20}$$

and for Darcy-Weisbach is written as

$$f^n_{i+\frac{1}{2}} = \begin{cases} 0 & \text{if } h_i = h_{i+1} = 0, \\ \dfrac{C_f u^n_{i+\frac{1}{2}} |u^n_{i+\frac{1}{2}}|}{8 g h^n_{i+\frac{1}{2}}} & \text{otherwise.} \end{cases}. \tag{21}$$

Meanwhile, the intermediate values $u^n_{i+\frac{1}{2}}$ and $h^n_{i+\frac{1}{2}}$ are defined by

$$u^n_{i+\frac{1}{2}} = \frac{h^n_{i+1} u^n_{i+1} + h^n_i u^n_i}{h^n_{i+1} + h^n_i}, \tag{22}$$

and

$$h^n_{i+\frac{1}{2}} = \frac{1}{2}(h^n_{i+1} + h^n_i), \tag{23}$$

respectively. Eventually, we can modify the reconstruction of Eqs. (16) - (18) become

$$h_{i+\frac{1}{2}L} = (h^n_i - (\Delta Z_{\text{app}})_+)_+, \tag{24}$$

$$h_{i+\frac{1}{2}R} = (h^n_{i+1} - (-\Delta Z_{\text{app}})_+)_+ \tag{25}$$

$$\Delta Z_{\text{app}} = \Delta Z + \Delta F_{i+\frac{1}{2}} \tag{26}$$

where ΔZ is defined by Eq. (18).

Remark 3.1. *Second-order. To improve the order of accuracy into higher order in the numerical scheme, we can use for instance the MUSCL reconstruction for space and Heun method for time. The detail about this method can be found in Bouchut (2004) and Delestre (2010).*

3.3. Numerical flux

As we already mentioned in previous section, we need to find the value of numerical flux $\mathcal{F}$. A general way to construct numerical flux $\mathcal{F}$ is the notion of approximate Riemann solver which come from the Godunov approach (Bouchut (2004)). Now we consider the initial data $U^n(x)$ which is piecewise constant, and we define an approximation solution for $t^n \leq t < t^{n+1}$ and $x \in \mathbb{R}$ by

$$U_{\text{appx}}(t,x) = R(\frac{x - x_{i+1/2}}{t - t^n}, U_i^n, U_{i+1}^n) \tag{27}$$

for $x_i < x < x_{i+1}$ with $x_i = (x_{i+1/2)+x_{i-1/2}})/2$. This approximation is possible until time t^{n+1} under a half CFL condition, in sense that

$$x/t < -\frac{\Delta x_i}{2\Delta t} \Rightarrow R(x/t, U_i, U_{i+1}) = U_i, \tag{28}$$

$$x/t > -\frac{\Delta x_{i+1}}{2\Delta t} \Rightarrow R(x/t, U_i, U_{i+1}) = U_{i+1}. \tag{29}$$

Then, the new values at time t^{n+1} are given as

$$U_i^{n+1} = \frac{1}{\Delta x_i} \int_{\Omega_i} U_{\text{appx}}(t^{n+1} - 0, x)\ \mathrm{d}x. \tag{30}$$

Note that our system is not conservative, however we can follow the same computations in Bouchut (2004), Chapter 2 to obtain

$$U_i^{n+1} = U_i^n - \vec{\xi}\frac{\Delta t}{\Delta x_i}\left(\mathcal{F}(U_i^n, U_{i+1}^n) - \mathcal{F}(U_{i-1}^n, U_i^n)\right). \tag{31}$$

Hence, by a relaxation approach of the coupled system of shallow water - Exner equations in Audusse et al. (2012), the numerical flux $\mathcal{F}$ is defined as

$$\mathcal{F}(U_l, U_r) = \begin{cases} F(U_l), & \text{if} \quad 0 \leq \sigma_1 \\ F(\hat{U}_l), & \text{if} \quad \sigma_1 \leq 0 \leq \sigma_2 \\ F(U_l^*), & \text{if} \quad \sigma_2 \leq 0 \leq \sigma_3 \\ F(U_r^*), & \text{if} \quad \sigma_3 \leq 0 \leq \sigma_4 \\ F(\hat{U}_r), & \text{if} \quad \sigma_4 \leq 0 \leq \sigma_5 \\ F(U_r), & \text{if} \quad 0 \leq \sigma_5 \end{cases} \tag{32}$$

where

$$F(U_l) = (h_l u_l, h_l u_l^2 + \Pi_l, Q_s(u_l))^T, \tag{33}$$

$$F(\hat{U}_l) = (\hat{h}_l \hat{u}_l, \hat{h}_l \hat{u}_l^2 + \hat{\Pi}_l, Q_s(\hat{u}_l))^T, \tag{34}$$

$$F(U_l^*) = (h_l^* u_l^*, h_l^* u_l^{*2} + \Pi_l^*, Q_s(u_l^*))^T, \tag{35}$$

$$F(U_r^*) = (h_r^* u_r^*, h_r^* u_r^{*2} + \Pi_r^*, Q_s(u_r^*))^T, \tag{36}$$

$$F(\hat{U}_r) = (\hat{h}_r \hat{u}_r, \hat{h}_r \hat{u}_r^2 + \hat{\Pi}_r, Q_s(\hat{u}_r))^T, \tag{37}$$

$$F(U_r) = (h_r u_r, h_r u_r^2 + \Pi_r, Q_s(u_r))^T, \tag{38}$$

with $\Pi = \frac{1}{2} g h^2$ and the waves speeds (see Fig. 2) are given by

$$\sigma_1 < \sigma_2 < \sigma_3 < \sigma_4 < \sigma_5, \tag{39}$$

with

$$\begin{aligned} &\sigma_1 = u_l - \frac{\beta}{h_l}, \sigma_2 = \hat{u}_l - \frac{\alpha}{\hat{h}_l}, \sigma_3 = u^*, \\ &\sigma_4 = \hat{u}_r + \frac{\alpha}{\hat{h}_r}, \sigma_5 = u_r + \frac{\beta}{h_r}. \end{aligned} \tag{40}$$

The superscripts ($\hat{}$) and (*) distinguish the intermediate and internal states respectively. In Fig. 2, we can see clearly that each wave separates the constant states: U_l, $\hat{U}_l$, U_l^*, U_r^*, $\hat{U}_r$, and U_r from the left to the right.

Moreover, according Audusse et al. (2012), to ensure the stability of the scheme, the parameter α and β are chosen such that $\alpha < \beta$. Hence, they are defined by

$$\alpha = \max_i \left(\sqrt{g h_i^3} \right), \tag{41}$$

$$\beta = \max \left(\max_i \left(\sqrt{(h_i u_i)^2 + g h_i^2 \partial_u (Q_s)_i} \right), \kappa \alpha \right). \tag{42}$$

where $i \in \mathbb{Z}$, and $\kappa > 1$. Further, in this paper we use $\kappa = 1.5$ for all numerical simulations.

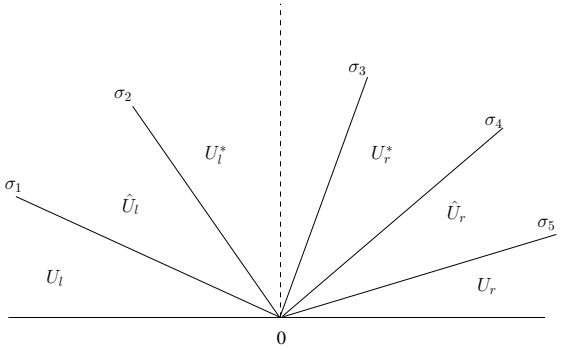

Figure 2: The Riemann solver for shallow water with a sediment layer.

According Audusse et al. (2012), the sediment elevation Z and sediment load Q_s are continuous through the intermediate and internal waves, because of the structure of the eigenvectors of the relaxation scheme. Therefore we define $\hat{Z}_l = Z_l^* = Z_r^* = \hat{Z}_r$ and $\hat{Q}_{sl} = Q_{sl}^* = Q_{sr}^* = \hat{Q}_{sr}$ as Z^* and Q_s^* respectively. The definition of the intermediate sediment elevation Z^* and

sediment load Q_s^* can be seen in Audusse et al. (2012)(Eqs. (15) and (16) respectively).

Finally the Courant-Friedrichs-Levy (CFL) condition of this scheme is given as

$$\Delta t = \nu \frac{\Delta x}{\max_i \sigma_i} \tag{43}$$

where $\nu \leq 1$ is a Courrant number.

In the end, we can summarize the previous information into an algorithm. It can be seen in Algorithm 1.

Algorithm 1 The hydrostatic relaxation scheme.

Step 1. Give the initial conditions at $n = 0$.

Step 2. Compute (41) and (42) to get α and β respectively.

Step 3. Compute Δt by (43) to preserve the stability.

Step 4. Solve (24) - (26) to apply the apparent topography for the friction term.

Step 5. Define the reconstructed states by (14) and (15).

Step 6. Compute the fluxes (12) and (13) with numerical flux $\mathcal{F}$ defined by (32) at each interface of cells.

Step 7. Finally, update the discrete value U_i^n into U_i^{n+1} by solving (11).

4. Numerical simulations

In this section we elaborate some numerical simulations such as the comparison between the analytical solution and the numerical scheme, transcritical flow over a granular bump, and the comparison water surface of dambreak over a granular bed with the data experiments. For all simulations,

the depth of bedrock to the reference level H is set to be constant, such that we have $\partial_x H = 0$.

4.1. Analytical solution

Here we consider the numerical simulation where the analytical solution is available. This simulation follow the paper of Berthon et al. (2012) with no friction term ($S_f = 0$).

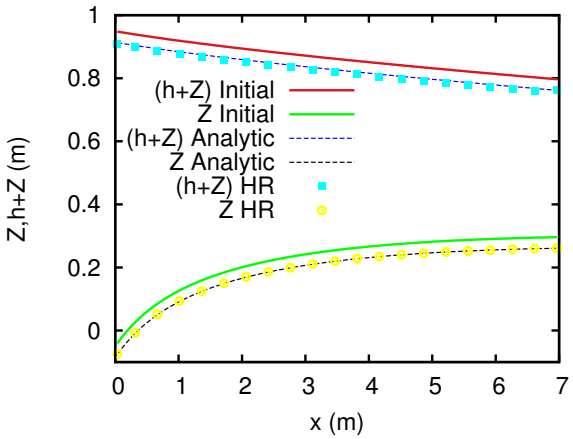

Figure 3: Comparison of hydrostatic relaxation (HR) scheme with the analytical solution at final time $t = 7$ s.

The space domain is $\Omega = [0, 7]$ and the initial conditions of this simulation are given by

$$(hu)_{\text{ini}}(x) = 1, \tag{44}$$

$$u_{\text{ini}}(x) = \left[\frac{ax + b}{A_g}\right]^{1/3}, \tag{45}$$

$$h_{\text{ini}}(x) = \frac{(hu)_{\text{ini}}(x)}{u_{\text{ini}}(x)}, \tag{46}$$

$$Z_{\text{ini}}(x) = 1 - \frac{u^3_{\text{ini}}(x) + 2g(hu)^2_{\text{ini}}(x)}{2gu_{\text{ini}}(x)}, \tag{47}$$

with coefficients $a = b$ both equal to 5×10^{-3}. The analytical solutions for h, u and Z can be found in the paper of Berthon et al. (2012).

In this simulation we consider the Grass formula with $Q_s = A_g u|u|^2$, where $A_g = 5 \times 10^{-3}$ and we used 100 grid points. In our simulation result, the scheme has a good behavior which is the convergence of our scheme is close to the analytical solution (see Fig. 3 and 4) even in coarse grids. Fig. 3 shows the free surface and sediment profile, and Fig. 4 shows the velocity profile at the final time $t = 7$ s. We can see clearly in velocity profile (Fig. 4), the hydrostatic relaxation (HR) scheme is less diffusive than the simple solver (SR) scheme obtained in Berthon et al. (2012).

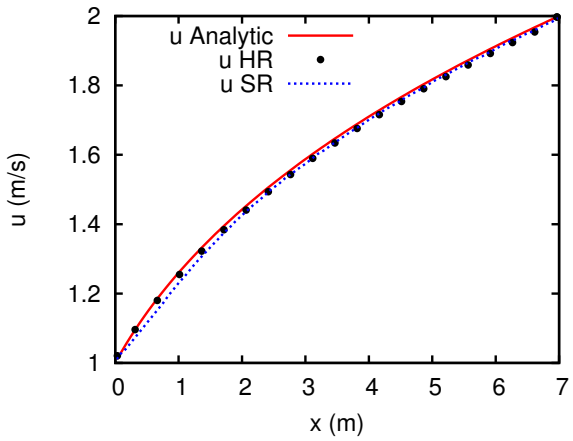

Figure 4: Comparison the velocity profile of hydrostatic relaxation (HR) scheme and simple solver (SR) scheme with the analytical solution at final time $t = 7$ s.

Tabel 1 collects the discrete L^1-norm errors for h, u, and Z at the final time with difference mesh sizes. Moreover, Tabel 1 also shows the rate of convergence for first-order computations, computed by comparison between two discrete L^1-norm errors with different mesh sizes. Here, we can confirm

Table 1: L^1-norm error of relaxation scheme at $t = 7$ s.

Cells	$\|\|h - h_{\text{analytic}}\|\|_{L^1}$	τ_h	$\|\|u - u_{\text{analytic}}\|\|_{L^1}$	τ_u	$\|\|Z - Z_{\text{analytic}}\|\|_{L^1}$	τ_Z
25	1.627E-1	/	2.266E-1	/	1.340E-2	/
50	8.494E-2	0.938	1.186E-1	0.934	7.742E-3	0.792
75	5.742E-2	0.966	8.073E-2	0.949	5.532E-3	0.828
100	4.335E-2	0.978	6.130E-2	0.957	4.338E-3	0.845
125	3.480E-2	0.983	4.947E-2	0.960	3.584E-3	0.856
200	2.192E-2	0.983	3.141E-2	0.966	2.358E-3	0.890

that our scheme has a good convergence rate τ where it tends to 1 since computed in first-order for each unknown variables (h, u and Z). The CFL number used is 1 in this simulation.

4.2. Transcritical flow over a granular bump

Here, we consider the numerical simulation of subcritical and supercritical flow over a granular bump. Before we get the steady state solution, first we start with the initial conditions:

$$Z_{\text{ini}}(x) = 0.1 + 0.1e^{-(x-5)^2}, \tag{48}$$

$$(hu)_{\text{ini}}(x) = 0.6, \tag{49}$$

$$h_{\text{ini}}(x) + Z_{\text{ini}}(x) = 0.4, \tag{50}$$

$$A_g = 0. \tag{51}$$

where the boundary conditions are $(hu)(0,t) = 0.6$ and $h(0,t) = 0.4$ with the space domain $\Omega = [0, 10]$. The 100 points of grids are used and the CFL condition is set to be 1 in this simulation.

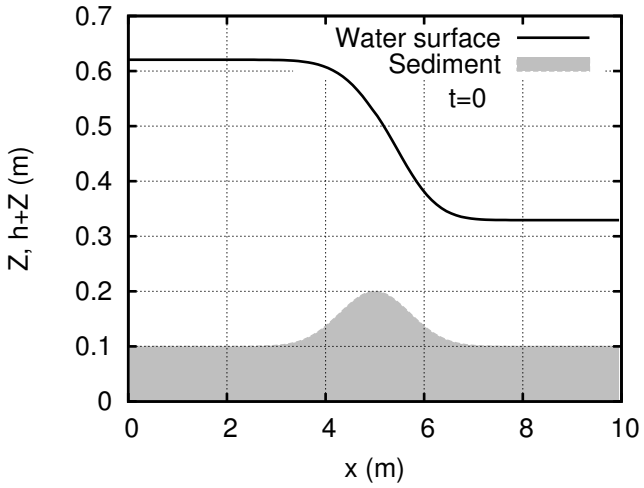

Figure 5: The initial condition of dam-break simulation over a granular bed

Once the steady state is reached (see Fig. 5), we set immediately the coefficient of Grass bedload flux with $A_g = 5 \times 10^{-4}$ hence the sediment could evolve in time.

As noted in Cordier et al. (2011), the important information is that in this simulation one can obtains a negative eigenvalue in supercritical regions. For instance, the splitting method does not take into account about this information, hence the instability occurs in the simulation (see Fig. 15 in paper of Cordier et al. (2011)). However, with our scheme (even in coarse grid and CFL =1) the simulation remains stable. The results in various final times $t = 15$ and $t = 30$ are shown in Fig. 6 and 7 respectively.

4.3. Dam-break over a granular bed

This simulation, we introduce the numerical experiment of dam-break flow over a granular bed. In Capart & Young (1998), the laboratory experiment has been done by mobile bed measurement 1.20 m long with 6 cm deep

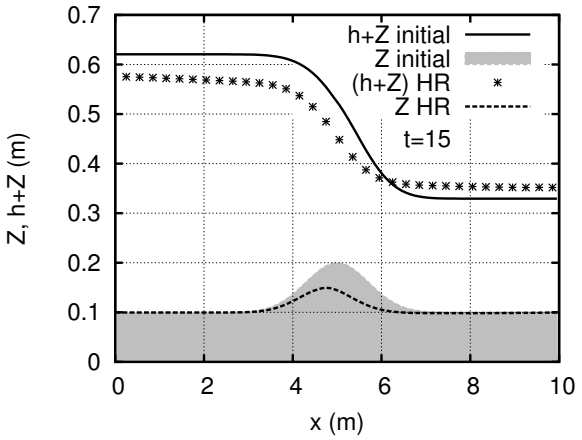

Figure 6: The solution of transcritical flow over a granular bed with $A_g = 5 \times 10^{-4}$ at final time $t = 15$

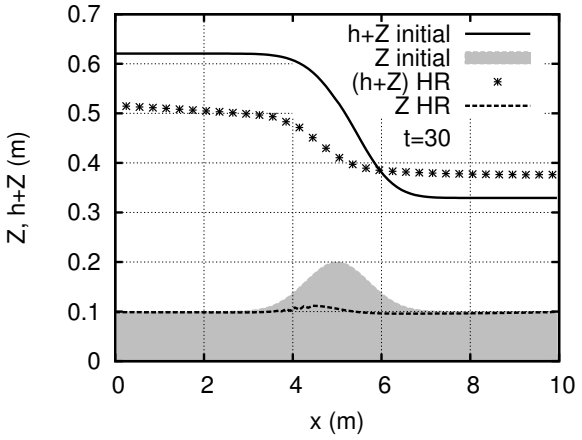

Figure 7: The solution of transcritical flow over a granular bed with $A_g = 5 \times 10^{-4}$ at final time $t = 30$

of particle layer. The dam is located at the left of domain with height and width are set to be 0.1 m and 0.4 m respectively (see Fig. 8).

In this simulation we used 100 points of gird and the parameters are $A_g = 0.01$, $g = 9.8$ m/s^2 and CFL condition is 1. The sequence comparisons

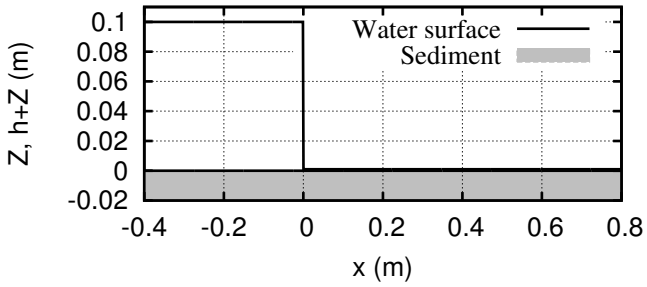

Figure 8: The initial condition of dam-break simulation over a granular bed

of our numerical scheme and data experiment in several final times are shown in Fig. 9. With hydrostatic relaxation scheme, we can see that our scheme has a good agreement with the rarefaction wave of dam-break. In the shock area, our numerical results are far away from the experiment data. However it is reasonably well since in the real experiment the sediment and water mixed in that area. Overall we can conclude that, the comparisons of numerical scheme and experiment observation are equitable well.

In the previous simulations, we consider the physical parameters of sediment such as, the diameter of sediment, porosity, friction etc into one constant value A_g by Grass formula. When we want to consider about the characteristics of sediment directly into simulation, the Grass formula is not suitable. Hence the Meyer-peter and Müller's formula is acceptable for that problem. In Wu & Wang (2007); Capart & Young (1998), two experiments on dam-break flow over movable beds which are performed in Taipei (University of Taiwan) and Louvain-la-Neuve (Uinversité Catholique de Louvain) have reported. In their report, the information about the characteristics of sediment are written in detail. Therefore, it will also be interesting if we compare our numerical simulation using the Meyer-peter and Müller's formula

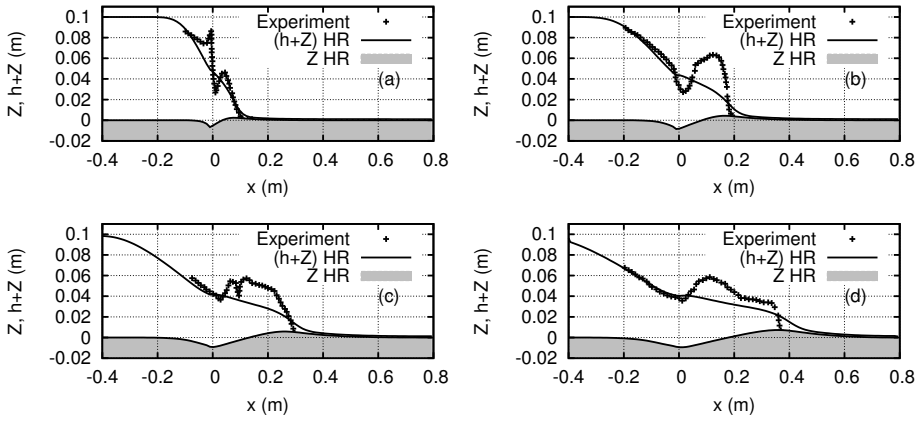

Figure 9: Comparison of water surface using hydrostatic relaxation scheme and data experiment by Capart & Young (1998): (a) dimensionless time $t = 1t_0$; (b) $t = 2t_0$; (c) $t = 3t_0$; and (d) $t = 4t_0$, where $t_0 = \sqrt{g/h_0}$, $h_0 = 0.1$ m.

with the data experiments given in Fraccarollo & Capart (2002).

In Fig. 10, we show the series of comparison of our numerical computation and data experiment by Louvain-la-Neuve experiment only. The characteristics of sediment are given similar as in Wu & Wang (2007). The sediment porosity $\phi = 0.3$, the diameter of sediment $d = 3.2$ mm, the density of sediment $1,540$ kg/m^3, and the Manning's coefficient 0.001 and 0.025 are given for water and sediment respectively. The domain of this simulation is $\Omega = [-1.25 : 1.25]$, the initial conditions are

$$h_{\text{ini}}(x) = h_0 \mathbb{1}_{x<0},$$
$$Z_{\text{ini}}(x) = 0,$$
$$u_{\text{ini}}(x) = 0,$$

where the initial water depth $h_0 = 0.1$ m.

195 Fig. 10 shows the nice comparison of our numerical simulation and data

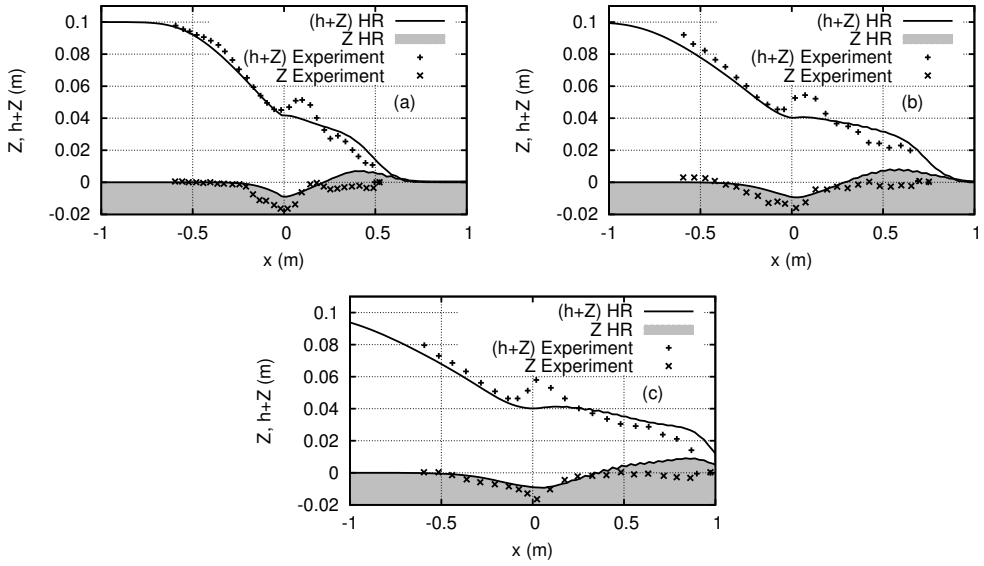

Figure 10: Comparison of water surface using hydrostatic relaxation scheme and data experiment in Louvain case: (a) dimensionless time $t = 3t_0$; (b) $t = 7.5t_0$; and (c) $t = 10t_0$, where $t_0 = \sqrt{g/h_0}$, $h_0 = 0.1$ m.

experiment both in water height and sediment profile. Thus our scheme is capable to handle simulation when considering the physical characteristic of sediment.

5. Conclusion

In the present study, we introduced the hydrostatic relaxation scheme to approximate the shallow water-Exner equations. This scheme is based on the hydrostatic reconstruction and relaxation solver. The relaxation solver was introduced in Audusse et al. (2012), and is stable and well-posed for shallow water-Exner equations. Further we modify their scheme by using hydrostatic reconstruction on their solver, which enabled us to get better numerical results. Indeed, some numerical experiments show the robustness and accurateness of the scheme. The comparison of numerical results with the analytical solution and data experiments are obtained nicely comparable. Additionally, the convergence properties to an analytical solution is satisfied (the convergence rate tends to 1 in discrete L^1-norm errors since the first order scheme is applied). The scheme also shows efficient and as well as stable even in stiff conditions. Moreover, this scheme is simple and robust, therefore it is flexible for many applications. Finally, the comparison between this paper and the papers of Cordier et al. (2011) and Audusse et al. (2012) are drawn up in Table 2.

References

Audusse, E., Berthon, C., Chalons, C., Delestre, O., Goutal, N., Jodeau, M., Sainte-Marie, J., Giesselmann, J., & Sadaka, G. (2012). Sediment trans-

Table 2: The comparison between this paper and the papers of Cordier et al. (2011) and Audusse et al. (2012).

	This paper	Cordier et al. (2011)	Audusse et al. (2012)
Numerical method:	Hydrostatic reconstruction + Relaxation solver	Coupled Roe scheme	Relaxation simple solver
Comparison of numerical results and analytical solution by Berthon et al. (2012)	Done	Undone	Done
Table L^1-norm error	Done	Done	Undone
Dam-break over a granular bed simulation	Done	Undone	Done
Transcritical flow over a granular bump simulation	Done	Done	Undone
Comparison between dam-break over a granular bed simulation and data experiments	Done	Undone	Undone

port modelling: Relaxation schemes for saint-venant–exner and three layer models. In *ESAIM: Proceedings* (pp. 78–98). EDP Sciences volume 38. doi:10.1051/proc/201238005.

Audusse, E., Bouchut, F., Bristeau, M.-O., Klein, R., & Perthame, B. (2004). A fast and stable well-balanced scheme with hydrostatic reconstruction for shallow water flows. *SIAM Journal on Scientific Computing*, *25*, 2050–2065. doi:10.1137/S1064827503431090.

Berthon, C., Cordier, S., Delestre, O., & Le, M. H. (2012). An analytical solution of the shallow water system coupled to the exner equation. *Comptes Rendus Mathematique*, *350*, 183–186. doi:10.1016/j.crma.2012.01.007.

Bouchut, F. (2004). *Nonlinear Stability of Finite Volume Methods for Hyperbolic Conservation Laws: And Well-Balanced Schemes for Sources*. Frontiers in Mathematics. Birkhäuser Verlag, Basel.

Bouchut, F., SOMMER, J., & Zeitlin, V. (2004). Frontal geostrophic adjustment and nonlinear wave phenomena in one-dimensional rotating shallow water. part 2. high-resolution numerical simulations. *Journal of Fluid Mechanics*, *514*, 35–63. doi:10.1017/S0022112004009991.

Cao, Z., Pender, G., & Meng, J. (2006). Explicit formulation of the shields diagram for incipient motion of sediment. *Journal of Hydraulic Engineering*, *132*, 1097–1099. doi:10.1061/(ASCE)0733-9429(2006)132:10(1097).

Cao, Z., Pender, G., Wallis, S., & Carling, P. (2004). Computational dam-break hydraulics over erodible sediment bed. *Journal of hydraulic engineering*, *130*, 689–703. doi:10.1061/(ASCE)0733-9429(2004)130:7(689).

Capart, H., & Young, D. (1998). Formation of a jump by the dam-break wave over a granular bed. *Journal of Fluid Mechanics*, *372*, 165–187. doi:10.1017/S0022112098002250.

Cordier, S., Le, M. H., & Morales de Luna, T. (2011). Bedload transport in shallow water models: Why splitting (may) fail, how hyperbolicity (can) help. *Advances in Water Resources*, *34*, 980–989. doi:10.1016/j.advwatres.2011.05.002.

Delestre, O. (2010). *Simulation du ruissellement d'eau de pluie sur des surfaces agricoles*. Ph.D. thesis Université d'Orléans.

Delestre, O., Lucas, C., Ksinant, P.-A., Darboux, F., Laguerre, C., Vo, T.-N., James, F., Cordier, S. et al. (2013). Swashes: a compilation of shallow water analytic solutions for hydraulic and environmental studies. *International Journal for Numerical Methods in Fluids*, *72*, 269–300. doi:10.1002/fld.3741.

Doyen, D., & Gunawan, P. H. (2014). An explicit staggered finite volume scheme for the shallow water equations. In *Finite Volumes for Complex Applications VII-Methods and Theoretical Aspects* (pp. 227–235). Springer. doi:10.1007/978-3-319-05684-5_21.

Fraccarollo, L., & Capart, H. (2002). Riemann wave description of erosional dam-break flows. *Journal of Fluid Mechanics*, *461*, 183–228. doi:10.1017/S0022112002008455.

Greenberg, J. M., & Leroux, A.-Y. (1996). A well-balanced scheme for the

numerical processing of source terms in hyperbolic equations. *SIAM Journal on Numerical Analysis*, *33*, 1–16. doi:10.1137/0733001.

Herbin, R., Kheriji, W., & Latché, J. C. (2014). On some implicit and semi-implicit staggered schemes for the shallow water and euler equations. *ESAIM: Mathematical Modelling and Numerical Analysis*, *eFirst*, 1290–3841. doi:10.1051/m2an/2014021.

Julien, P., & Simons, D. (1985). Sediment transport capacity of overland flow. *Transactions of the ASAE*, *28*, 755–762. doi:10.13031/2013.32333.

Kadlec, R. H. (1990). Overland flow in wetlands: vegetation resistance. *Journal of Hydraulic Engineering*, *116*, 691–706. doi:10.1061/(ASCE)0733-9429(1990)116:5(691).

LeVeque, R. J. (1998). Balancing source terms and flux gradients in high-resolution godunov methods: the quasi-steady wave-propagation algorithm. *Journal of computational physics*, *146*, 346–365. doi:10.1006/jcph.1998.6058.

Rijn, L. C. v. (1984). Sediment transport, part ii: Suspended load transport. *Journal of Hydraulic Engineering*, *110*, 1613–1641. doi:10.1061/(ASCE)0733-9429(1984)110:11(1613).

Simpson, G., & Castelltort, S. (2006). Coupled model of surface water flow, sediment transport and morphological evolution. *Computers & Geosciences*, *32*, 1600–1614. doi:10.1016/j.cageo.2006.02.020.

Stelling, G., & Duinmeijer, S. (2003). A staggered conservative scheme for every froude number in rapidly varied shallow water flows. *International*

Journal for Numerical Methods in Fluids, *43*, 1329–1354. doi:10.1002/fld.537.

Tang, H., Tang, T., & Xu, K. (2004). A gas-kinetic scheme for shallow-water equations with source terms. *Zeitschrift für angewandte Mathematik und Physik ZAMP*, *55*, 365–382. doi:10.1007/s00033-003-1119-7.

Tao, T., & Xu, K. (1999). Gas-kinetic schemes for the compressible euler equations: positivity-preserving analysis. *Zeitschrift für angewandte Mathematik und Physik ZAMP*, *50*, 258–281. doi:10.1007/s000330050150.

Van Rijn, L. C. (1984). Sediment transport, part i: bed load transport. *Journal of hydraulic engineering*, *110*, 1431–1456. doi:10.1061/(ASCE)0733-9429(1984)110:10(1431).

Wu, W., & Wang, S. S. (2007). One-dimensional modeling of dam-break flow over movable beds. *Journal of hydraulic engineering*, *133*, 48–58. doi:10.1061/(ASCE)0733-9429(2007)133:1(48).